A quantitative assessment of human interventions and climate change on the West African sediment budget

A. Giardino[a,*], R. Schrijvershof[a], C.M. Nederhoff[a], H. de Vroeg[a], C. Brière[a], P.-K. Tonnon[a], S. Caires[a], D.J. Walstra[a,b], J. Sosa[c], W. van Verseveld[a], J. Schellekens[a,d], C.J. Sloff[a,e]

[a] *Deltares, Unit Marine & Coastal Systems, Boussinesqweg 1, 2629 HV Delft, The Netherlands*
[b] *Delft University of Technology, Faculty of Civil Engineering and Geosciences, The Netherlands*
[c] *University of Bristol, Bristol, United Kingdom*
[d] *Vrije Universiteit Amsterdam, Department of Hydrology and Geo-environmental Sciences, The Netherlands*
[e] *Delft University of Technology, Faculty of Hydraulic Engineering, The Netherlands*

A B S T R A C T

The West African coastal barrier is maintained by significant wave-driven longshore sand transport. This sand originates from rivers and large coastal sand deposits. Today, however, much of the fluvial sand is trapped behind river dams and/or interrupted at several locations by port jetties. As a result, the sandy coastal barrier is eroding almost everywhere along its length.

The aim of this study is to derive a large-scale sediment budget analysis, following a consistent approach, for the following countries: Republic of Côte d'Ivoire, Ghana, Togo and Benin, and pointing out the effects of major human interventions and climate change in this large common sediment system. The results are used as a basis to raise awareness among local governments and organizations on the effects and interdependency that major anthropogenic interventions (i.e. port jetties and river dams) and climate change (i.e. sea level rise, changes in wave climate, precipitation and temperature) may have on this shared sediment system. These detrimental effects can even occur in neighboring countries, as shown by some of the results. This estimation was carried out using a quantitative approach, based on one consistent numerical modelling system and validated with regional and local data.

Based on the outcomes of the study, and with the support of a number of validation workshops in the different countries, suggestions are also provided for the setting up of a regional sediment management plan for the entire region.

1. Introduction

Coastal areas and deltas around the world consist of sediments, which are mainly supplied by rivers that transport them from upstream catchments. Sediments are transported in a dynamic way as they move down rivers and along the coast, driven by the predominant flow conditions.

This transport is essential to keep coastlines in morphodynamic equilibrium. However, an unbalance between sediment supply and demand may lead to the erosion of coastal sections that were historically stable. The dominant factors which affect sediment balance are shown in Fig. 1. The most important anthropogenic interventions are major river dams, ports, coastal protection works, and sand mining activities. In addition, other factors affecting the coastal sediment budget are the presence of submarine canyons close to the coastline, but

also sea level rise and climate change (Syvitski et al., 2009).

The West African coast is a typical example where, nowadays, most fluvial sand is retained behind river dams and/or interrupted at several locations by port jetties. As a result, the sandy coastline is eroding almost everywhere. This coastal zone is also home to about 31% of the West Africa's population, and this figure is expected to rise. Urban population growth in the region is increasing at an annual rate of 4% (i.e. almost twice the worldwide average) (World Bank, 2016). Moreover, the problem becomes even more critical when considering that the coastal zone is the source of 56% of West Africa's GDP.

The problem of coastal erosion was investigated by UNEP in 1985 (UNEP, 1985). Since then, numerous studies have been undertaken (Tilmans et al., 1991; Allersma and Tilmans, 1993; Degbe, 2009). In particular, UEMOA (2011, 2015) has carried out a regional study for shoreline monitoring with the goal of developing a management plan
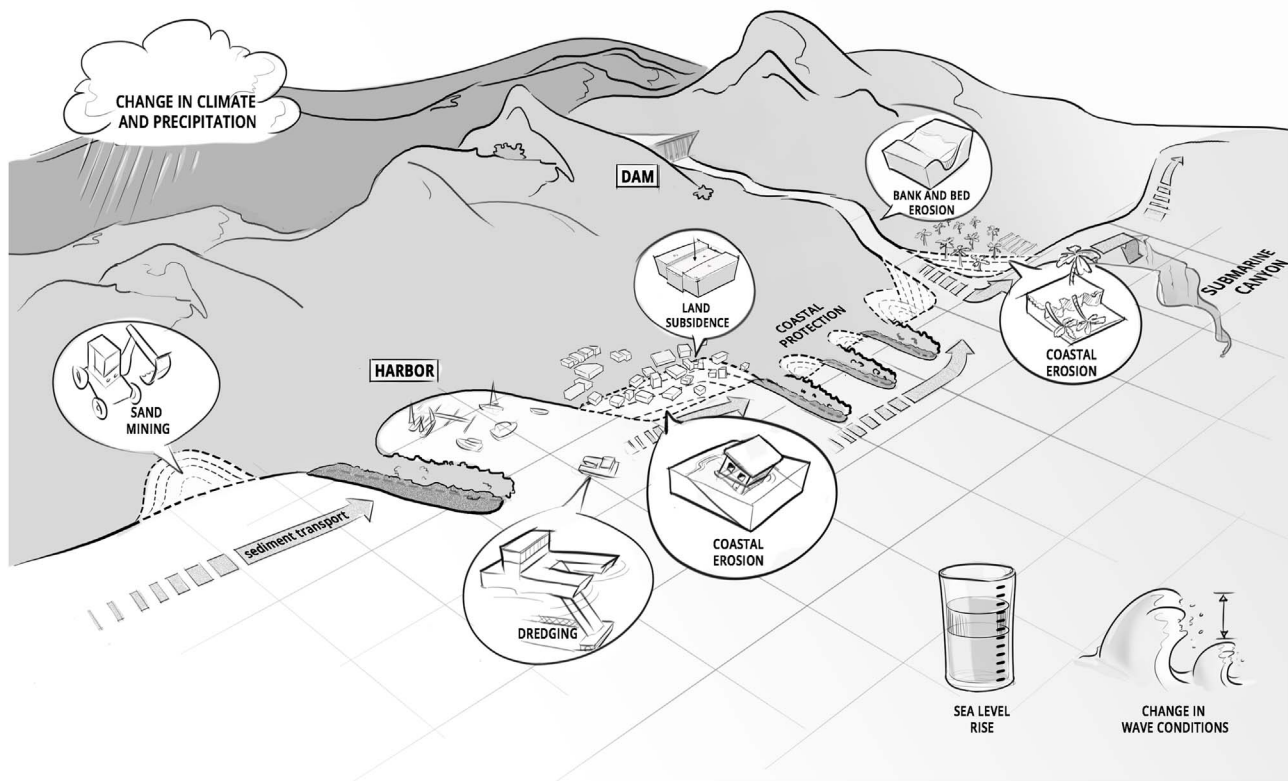
Fig. 1. Major factors which may affect the sand river and consequent morphological changes.

for the coastal area.

Wognin (2004), Abe (2005), and Wognin et al. (2013) described the shoreline changes in Côte d'Ivoire. In particular, using satellite images and photography, Wognin et al. (2013) showed how the port of Abidjan was responsible for erosion rates of about 1.5 m/year on the lee-side of the structure.

Changes in coastline position in Ghana were assessed by Ly (1980), Wiafe (2011) and Boateng (2012). Ly (1980) pointed out the role of the Akosombo dam and also the ports on the observed shoreline changes. Wiafe (2011) used satellite remote sensing to propose a zonation of the coastline, characterized by different rates of shoreline changes. The author stated that the Western Ghana is eroding at an average rate of 1.58 m/year, with a considerable variation along the coast. Boateng (2012) carried out a study based on GIS techniques and field observation covering 203 km of the 540 km Ghana coastline. Averaged erosion values were found ranging between 1.6 m/year in the western part, 2.7 m/year in the central part, and 3.9 m/year in the eastern part. Jonah et al. (2015) assessed the yearly sediment loss and consequent coastal erosion due to beach sand mining activities along the coastline of Cape Coast. According to the authors, sand mining is the main cause of erosion along the coastline of Cape Coast.

The coastal system in the Bight of Benin (i.e. which include Togo and Benin) have been largely influenced by the construction of the Akosombo dam on the Volta River in 1961 and the construction of the deepwater port of Lomé (Anthony and Blivi, 1999). Laïbi et al. (2014) pointed out how the deepwater ports constructed in the Bight of Benin and the Akosombo dam resulted in the destabilization of the former single drift cell on this coast. Kaki et al. (2011) discussed the evolution of the coastline in Benin as a result of the construction of the port of Cotonou. The study is based on detailed analysis of remote sensing data

and verified with ground truthing, for period 1963 up to 2005. Shoreline changes of nearly 500 m were observed within the period of observation (i.e. accretion west of the port and erosion on the eastern side).

Although these previous studies are valuable as a first assessment of the on-going erosion problems, no consistent overall analysis of the regional sediment budget of the West African coastal system is available. The present study's main objective is to develop a quantitative and consistent large-scale sediment budget for the West African coastal system (i.e. Côte d'Ivoire, Ghana, Togo and Benin) based on a single numerical modelling framework. The study provides quantitative information of the potential longshore sediment transport, assuming sufficient sediment supply. Furthermore, the modelling framework is utilized to provide estimates of the effects that major man-made interventions and climate change may have on this potential longshore sediment transport and consequent shoreline changes.

The paper comes with a freely available database of nearshore wave conditions for the entire West African coast:

http://opendap.deltares.nl/thredds/catalog/opendap/deltares/publications/Giardino_2017/catalog.html
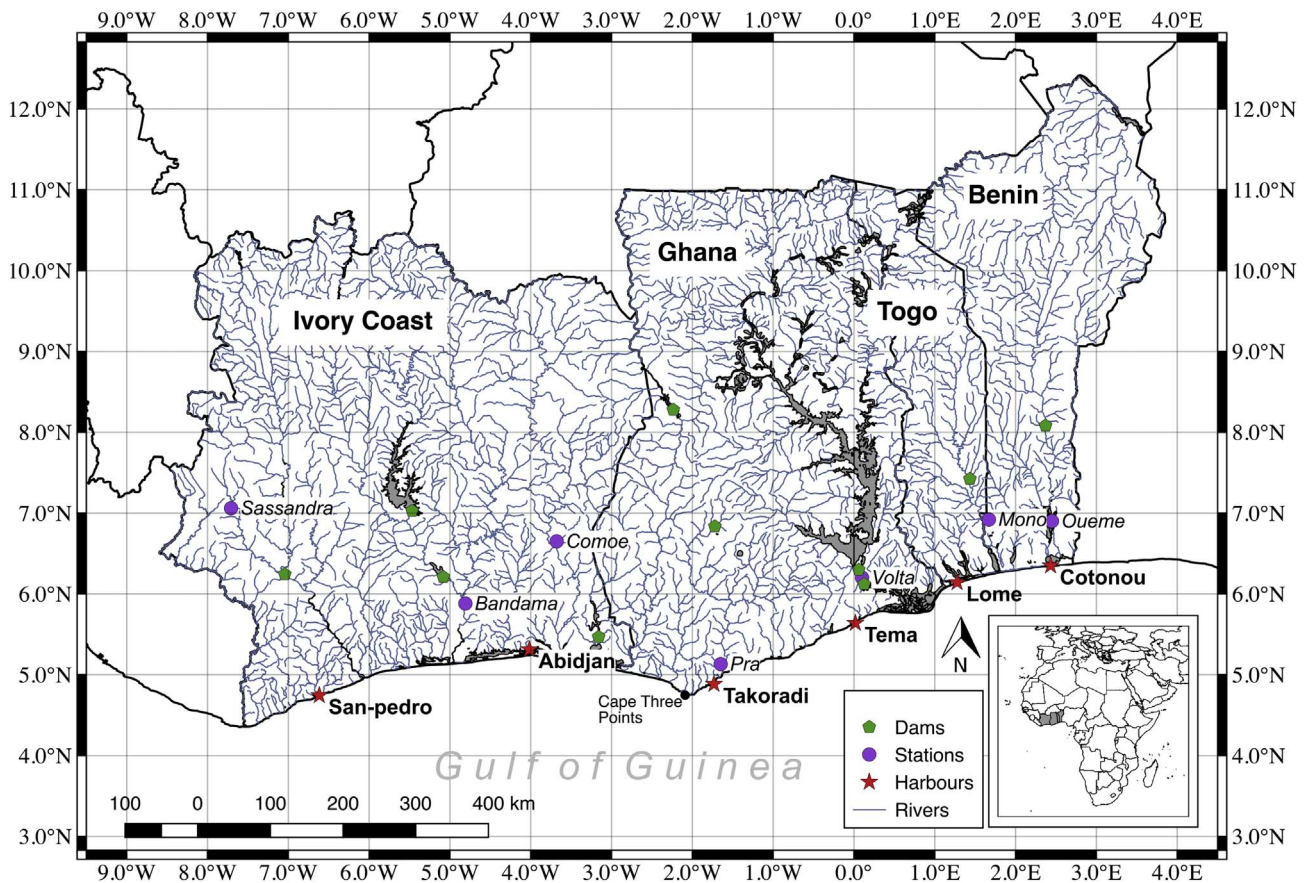
and a coastal viewer:

http://v-web004.deltares.nl/africa/africa/

Fig. 2. Geographical location of the study area, with locations of the main anthropogenic interventions in the region, at the coast and on the main rivers.

2. Materials and methods

2.1. Study area

Côte d'Ivoire, Ghana, Togo and Benin are located on the West African coast (Fig. 2). In the South, the countries are bordered by the Gulf of Guinea, while in the North they are backed by the African continent, from which several rivers originate and descend into the ocean. The total length of the coastline is about 1300 km, ranging approximately between 7.5°W and 2.7°E in longitude, and developing around the 5–6°N parallel.

Two main geomorphological units can be distinguished: the concave coast between Cape Palmas and Cape Three Points in Côte d'Ivoire and Ghana (≈ from long. 7.5°W to 2°W) and the coast from Cape Three Points on the border between Benin and Nigeria (≈ from long. 2°W to 2.7°E), which continues until the Niger delta.

The continental shelf is narrow, with widths of 20–25 km along Côte d'Ivoire and the coasts of Togo and Benin, and 20–80 km between Cape Three Points and the Volta Delta. A submarine canyon exists off the Canal de Vridi in Côte d'Ivoire, the so-called "Trou Sans Fond" (long. ≈ 4°W). Generally, the coastal area is low, with the 100-m contour at a distance of 25–100 km inland (Allersma and Tilmans, 1993). Steeper coasts with rocky outcrops and pocket beaches exist in the most western part, between approximately longitude 7.5°W and 5.8°W, and between approximately 2.3°W to 1.6°W.

The Guinea current flows offshore from west to east. Its mean velocity varies between 1 m/s (max. 1.5 m/s) in summer, and 0.5 m/s (max. 0.75 m/s) in winter and it becomes weaker moving east (Allersma and Tilmans, 1993). The phase of the semi-diurnal tide is uniform along the coast, with an average range of about 1 m. The wind climate is generally characterized by a persistent south-westerly monsoon modified by land and sea breezes in the coastal area. Waves

reaching the coast have two main origins: wind-waves generated by the weak, local monsoon; and swell-waves, generated by storms in the southern part of the Atlantic Ocean. The average significant wave height is 1.36 m with a peak period of 9.4 s and a dominant South-South West Direction (189°) (Almar et al., 2015). The seasonal modulation of swell waves is weak, with wave height peaking at 1.6 m during austral winter. On the contrary, the annual average wind wave height is smaller (0.4 m) and the direction is more oriented from the west (215°).

Allersma and Tilmans (1993) reported values of longshore sediment transport generally eastward directed, and ranging between 0 up to 1.2 million m^3/year, depending on the location. Values within the same order of magnitude have been reported by other authors (e.g. Tilmans et al. (1995); Anthony (1995); Anthony and Blivi (1999); Almar et al. (2015). According to Almar et al. (2015), the contribution of swell waves to gross annual longshore transport is one order of magnitude larger than that due to wind-waves. In all these studies, estimates of longshore transport are based on simple empirical formula or measurements of shoreline evolution near major port breakwaters. Neither a full wave modelling study for the entire study area, nor a comprehensive sediment transport and shoreline model were used in the previous studies.

The climate along the coast of West Africa is equatorial, with considerable differences in the amount and seasonal distribution of the precipitation (Allersma and Tilmans, 1993). Rains of more than 2000 mm per year feed tropical rain forests along Côte d'Ivoire and in West Ghana. There are two maxima (May–June and October–November). The eastern part of the coastline is considerably drier than the western part. From West to East, the main rivers contributing to the coastal sediment budget are: Sassandra, Bandama and Comoé (Côte d'Ivoire), Pra, Volta (Ghana), Mono (Togo), Oueme (Benin). The Volta River has, by far, the largest discharge of all other rivers in the region.

According to Anthony et al. (2016), the discharge varied between a low of 1000 m^3/s in the dry season and a high of over 6000 m^3/s in the wet season before completion of the Akosombo dam.

2.2. Overview of the main anthropogenic interventions

In this section, the most important anthropogenic interventions which have impacted this sediment balance are described: ports and river dams.

Other forms of anthropogenic intervention may also modify the coastal sediment budget, for example: changes in land use in the river basins, local dredging and dumping of sand, coastal defences (e.g. groynes, seawalls, nourishments, etc.). However, those types of interventions have not been considered as part of this study.

2.2.1. Main ports

The general effect of harbour jetties on the shoreline evolution is to block (part of) the longshore transport, inducing accretion at the upstream side of the structure and erosion on the leeside. In addition, more complex two-dimensional effects can be observed close to the harbour.

Several ports have been built during the years along the coast of Côte d'Ivoire, Ghana, Togo and Benin. An overview of the main ports is shown in Table 1.

2.2.2. Interventions on the main rivers

River dams affect the coastal sediment budget in different ways. Rivers tend to carry sediment from the upstream catchments, allowing for the formation of depositional features such as river deltas, alluvial fans, braided rivers, and beaches. The construction of a river dam first of all will reduce or block the flow of sediment downstream of the dam. The direct consequence is downstream erosion, which can extend for tens of kilometres downstream of the dam. In addition, river dams also modify the hydrograph of the rivers (e.g. decreasing the peaks in river flows and increasing the base flow). Peaks in river flows generally bring the largest contribution of sediment downstream and, in particular, the coarsest fraction. This coarsest sand and gravel fraction is often the most important building component of many beaches around the world (see e.g. Giardino et al., 2015). An overview of the main dams built within the study area is given in Table 2.

2.3. Input data

2.3.1. Bathymetry

The depth information was obtained primarily from the GEBCO (General Bathymetric Charts of the Ocean, http://www.gebco.net/) global bathymetric data sets. The GEBCO's gridded bathymetric data sets are global terrain models for ocean and land; data is provided at a global 30 arc-second interval grid. In order to improve the data accuracy in the area closer to the coast, the depth information was supplemented with higher resolution data retrieved after digitalization of several admiralty charts (num. 1362, 3100, 1383, and 1384).

Table 1
Overview of the main ports within the study area.

Main ports	Country	Date of construction
San-Pédro	Côte d'Ivoire	1970
Abidjan	Côte d'Ivoire	1951
Takoradi	Ghana	1928
Takoradi ports extension	Ghana	1955
Tema	Ghana	1961
Lomé	Togo	1968
Cotonou	Benin	1963

2.3.2. Wind and waves

ECMWF (European Centre for Medium-Range Weather Forecasts, http://www.ecmwf.int/en/research/climate-reanalysis/era-interim) ERA-Interim wind and wave data were used in this study. In particular, the most recent reanalysis of these data (Dee et al., 2011). The data are 6 hourly, starting from 1979 and are available on a global grid with a resolution of about 0.75° × 0.75°. The data contain information on wind speed (U10), wind direction as well as on wave conditions (i.e. wave height, period and direction).

Altimeter data were used for calibration of the ERA-Interim dataset. As a consequence of this calibration, ERA-Interim wave heights were increased by 10% while the wave periods were increased by 4.8%.

Fig. 3 shows the wave roses off the West African coast derived based on the ERA-Interim dataset. The figure clearly shows that most of the waves are directed from southerly direction with a clockwise rotation moving towards the east.

2.3.3. Shoreline evolution data based on satellite images

Shoreline evolution data were derived based on Landsat Satellite Images, using an automated procedure that detects the presence of water or land (Donchyts et al., 2016). Those data were used for calibration of the shoreline model. In particular, satellite data near major ports were analyzed for the period 1985–2015 and compared with the output from model data, using the 1985 as reference shoreline. Future shoreline changes were predicted by using the 2015 shoreline as reference line.

2.3.4. Sea level rise

Sea level rise (SLR) affects the coastal sediment budget in multiple ways: on the one hand SLR leads to coastal recession in general which can be roughly estimated based on the Bruun rule (Bruun, 1962). According to the Bruun rule, the shoreface profile moves upward by the same amount as the rise in sea level, through erosion of the upper shoreface and deposition on the lower shoreface. The validity of the Bruun rule has been questioned in literature (e.g. Cooper and Pilkey, 2004; Ranasinghe et al., 2012) but it is still widely used for first order assessments of the effects of SLR such as in this study.

On the other hand, SLR also contributes to an increase in wave height due to a reduction in wave dissipation of waves propagating towards the shore.

In order to investigate the relative effects of SLR on the nearshore sediment budget, two scenarios were assessed. A lower scenario characterized by a SLR of +0.3 m and an upper scenario characterized by a SLR of +1.0 m. The first scenario roughly corresponds to a RCP (Representative Concentration Pathways; IPCC, 2013) 4.5 scenario (0.05 percentile), and the latter roughly corresponding to a RCP 8.5 scenario (95 percentile). In particular, SLR values at one location off the coast of Ghana for the year 2100 (−1.5°W, +3.5°N) were used.

2.3.5. Changes in wave conditions due to climate change

The effect of predicted changes in wave conditions was estimated based on Hemer et al. (2013). According to the study, an increase in wave height up to 3% and a clockwise rotation up to 2° can be expected by the end of the century for the time period 2070–2100 in the West Africa region, when compared to the present climate (time period 1979–2009).

2.3.6. Changes in temperature and precipitation due to climate change

Climate change may affect the future hydrology of the river catchments which, in turn, may impact the sediment input towards the coastal system. For example, an increase in temperature may lead to an increase in evapotranspiration and therefore lower river discharges and a decrease of transported sediment towards the coastal system. Furthermore, an increase in precipitation, according to Dendy and Bolton (1976), could lead to more extensive ground cover by vegetation and therefore lower sediment yields.

Table 2
Overview of the main river dams within the study area.

| Name of dam	Country	River	Sub-basin	"Operational since"	Reservoir capacity (10^6 m³)	Reservoir area (×1000 m²)	Latitude	Longitude
Ayme II	Côte d'Ivoire	Bia	Comoe	1964	69	1000	5.467	−3.161
Buyo	Côte d'Ivoire	Sassandra	Sassandra	1980	8300	895,000	6.241	−7.346
Kossou	Côte d'Ivoire	Bandama	Bandama	1972	27,675	1,780,000	7.031	−5.474
Taabo	Côte d'Ivoire	Bandama	Bandama	1979	621	29,700	6.231	−5.084
Akosombo	Ghana	Volta	Volta	1961	147,960	8,482,250	6.350	0.100
Barekese	Ghana	Ofin	Pra	1969	34	6400	6.836	−1.721
Bui	Ghana	Volta	Mouhoun	2013	12,570	444,000	8.182	−2.166
Kpong	Ghana	Volta	Volta	1981	200	25,200	6.119	0.125
Nangbeto	Togo	Mono	Mono	1987	1710	180,000	7.533	1.089
Ilauko	Benin	Ilauko	Oueme	1979	24		8.082	2.371
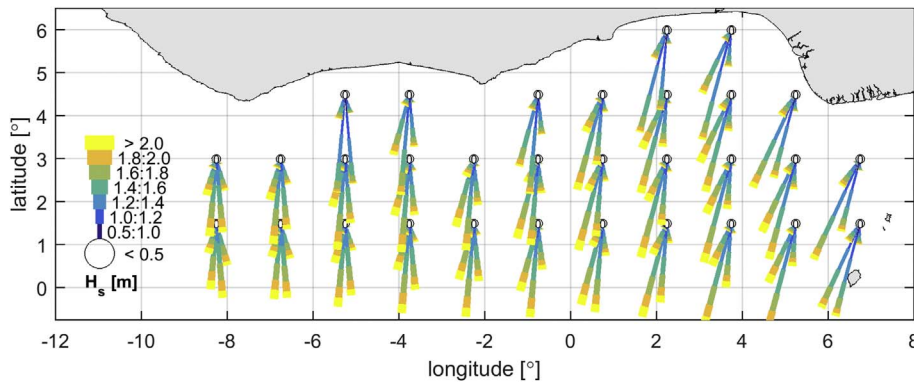
Fig. 3. Wave roses as derived from the ERA-Interim dataset.

In particular, the following processes related to climate change in the river catchments were investigated as part of this study: changes in temperature, precipitation and evapotranspiration.

2.3.6.1. Temperature. According to Christensen and Christensen (2007), the temperature may increase from 2° to 6° by 2100. In this paper, we consider an increase in temperature of 6° by 2100 for the period 2070–2100 as worst-case scenario.

2.3.6.2. Precipitation. Future trends in precipitation are under debate. Following Sultan et al. (2013) we consider two different scenarios, with an increase and a decrease of 20% respectively in precipitation for the period 2070–2100.

2.3.6.3. Potential evapotranspiration. The future potential evapotranspiration was estimated for the year 2100, according to the method described in Lu et al. (2005) and using as input the temperature at the end of the century as scaling parameter.

2.4. Numerical models

2.4.1. Modelling chain and simulated scenarios
The modelling chain includes:

- A set of nested wave models
- A sediment transport and shoreline evolution model, including the sediment input from the major rivers as source term to the coastal sediment budget

A list of the most relevant scenarios, is provided in Table 3. For a full description of all simulated scenarios the reader is referred to Giardino et al. (2017).

2.4.2. Wave modelling
The wave modelling was carried out with the Delft3D-WAVE (SWAN) model, (Holthuijsen et al., 1993; Booij et al., 1999). SWAN is a

Table 3
List of simulated scenarios.

Scenario description	Scenario name	Simulated period
Effects of man-made intervention	Hindcast simulation	1985–2015
	Reference scenario	2015–2045
	Major ports	2015–2045
	Major river dams	2015–2045
Effects of climate change	Changes in wave conditions	2070–2100
	Changes in temperature and precipitation in the river catchments	2070–2100
	Area loss due to SLR	2100

third-generation shallow water wave model, which solves the discrete spectral action balance equation. The model accounts for the effects of wind growth, wave dissipation due to whitecapping, bottom friction, wave breaking, non-linear wave-wave interactions, wave refraction and shoaling.

The wave propagation from offshore to nearshore was resolved based on one overall coarse model and 15 nested models, as shown in Fig. 4. The overall grid is set up in spherical coordinates (WGS84, EPSG: 4326) and extends from approximately −10 to +6° in longitude and between +3 and +6° in latitude. It has a grid size of approximately 1000 m in both cross-shore and longshore direction. The detailed grids have a finer resolution of 50 m in cross-shore and 100 m in longshore direction.

In order to determine the nearshore wave climate with limited computational time, the offshore wind and wave time series from the ERA-interim dataset was first reduced to a set of conditions representing the annual climate. In particular, wind and wave data time series were reduced to 139 separate classes, based on wave height (classes of 0.25 m), wave direction (classes of 10°) and wind direction (classes of 10°). Those conditions were propagated from offshore to nearshore based on separate stationary SWAN computations through the coarse model and the 15 nested models. Based on those conditions, relationships were established (i.e. transformation matrix), between
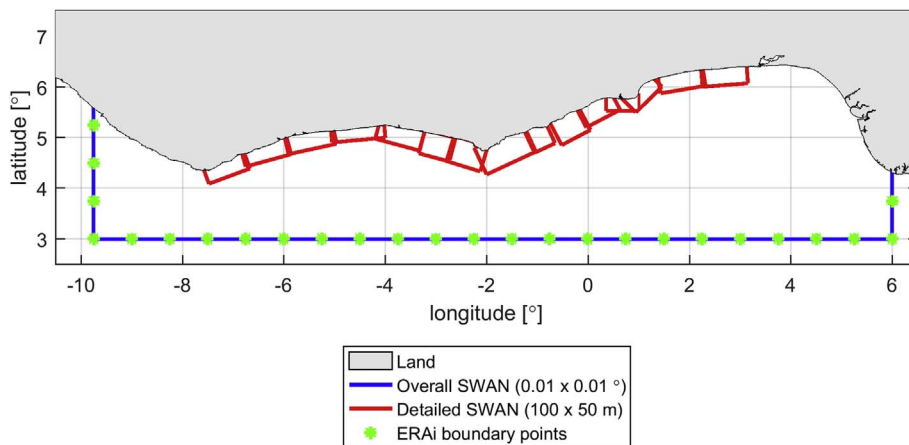
Fig. 4. Overview of the computational grids used for the wave modelling. Blue: overall grid; red: nested detailed grids. (For interpretation of the references to colour in this figure legend, the reader is referred to the Web version of this article.)

offshore conditions and nearshore conditions along the entire coast. Those relationships were applied to transform the complete offshore wave time series for the period 1979–2014 to nearshore, and finally used as input to the shoreline modelling.

2.4.3. Shoreline modelling

The longshore sediment transport and shoreline modelling was carried out with the UNIBEST-CL+ modelling package (Deltares, 2011). The model computes the potential longshore sediment transport generated by local wave and flow conditions, and as a function of coastal (e.g. coastal orientation, slope) and sediment (e.g. grain size) characteristics. The use of the term 'potential' here means that the model computes the volume of sand that *may* be moved longshore by the local hydrodynamic conditions, assuming that this volume of sand is available from upstream.

The shoreline evolution is then derived as a result of gradients in longshore transport. The longshore transport computations are executed for 72 selected locations along the West African coast, with wave input data extracted from the 15 detailed SWAN models. The direction, magnitude and distribution along the cross-shore profile of sediment transport are calculated for the 139 nearshore wave classes individually and then added up to determine the total net transport. Sediment transport computations are performed based on the Van Rijn-1992 sediment transport formula (Van Rijn, 1984a,b). According to this formula, the total transport consists of a bottom transport and a suspended transport component. Transport rates depend on the sediment characteristics as well as the shear stresses induced by the combined action of current and waves.

One uniform sediment size (D_{50} = 250 μm) was used for the entire region. This assumption was necessary given the large extension of the study area and in order to avoid discontinuities in the longshore transport and shoreline modelling computation.

2.4.4. Sediment input from rivers

Sediment input from the major rivers was included in the UNIBEST-CL+ model as source term. The sediment yield for each river basin was estimated based on the Dendy and Bolton (1976) formula, which relates the mean annual runoff and the catchment area to the sediment yield. The mean annual runoff for the different river catchments was computed based on a large-scale hydrological model, implemented in the distributed hydrological modelling platform wflow, based on the wflow_sbm code (Schellekens, 2013; Lopez Lopez et al., 2015; Jeuken et al., 2016). Forcing data for the hydrological simulations (i.e. precipitation and potential evapotranspiration) have been extracted from the WFDEI dataset (Weedon et al., 2014). The sediment inputs were compared to the values reported by Allersma and Tilmans (1993) showing values in the same order of magnitude (Table 4). In reality, only the coarser fraction (sand and gravel) of the total sediment load

Table 4
Sediment yield from the different rivers.

River name	Catchment (km^2)	Runoff (mm/yr)	Sediment yield (m^3/yr) Dendy and Bolton (1976).	Sand fraction (m^3/yr)	Sediment yield (m^3/yr) from Allersma and Tilmans (1993).
Sassandra	66,000	207.0	$1.08 * 10^6$	$1.08 * 10^5$	$2.88 * 10^6$
Bandama	91,000	82.4	$3.52 * 10^6$	$3.52 * 10^5$	$4.00 * 10^6$
Comoé	78,000	40.8	$3.26 * 10^6$	$3.26 * 10^5$	$2.94 * 10^6$
Pra	22,714	274.7	$0.70 * 10^6$	$0.70 * 10^5$	$0.88 * 10^6$
Volta	394,100	88.7	$6.78 * 10^6$	$6.78 * 10^5$	$9.38 * 10^6$
Mono	21,000	153.1	$1.00 * 10^6$	$1.00 * 10^5$	$0.81 * 10^6$
Ouémé	42,000	115.0	$1.77 * 10^6$	$1.77 * 10^5$	$1.31 * 10^6$

contributes to the sediment volume forming the beach. In this study, the sand fraction is assumed to be 10% of the total sediment yield estimated based on Dendy and Bolton (1976), and in line with other estimates from previous literature (Allersma and Tilmans, 1993). It has to be stressed that these values are just an estimate for all river catchments, as precise measurements of sediment load for all rivers in the region are not possible.

When the river flow enters a reservoir, its velocity and hence transport capacity are reduced and the sediment load is deposited in the reservoir. Often, more than 90% of the incoming sediment load is trapped and deposited in horizontal strata or thin bands across the bottom of the reservoir (Van Rijn, 2005). Different methods exist to operate and manage sedimentation in reservoirs, which also results in different trapping rates.

The major rivers in the study area have been dammed. The trapping efficiency of the major reservoirs was estimated by means of the Brune (1953) formula, based on the mean annual runoff and the reservoir capacity. The values were compared with values obtained based on the Brown (1944) formula. Estimated trapping efficiency values for all different dams are shown in Table 5. When different dams exist on the same river, the overall trapping efficiency is obtained by multiplying the trapping efficiency of each single dam. This trapping efficiency was used to scale the total sand fraction brought from the river towards the coast in the reference situation. This is an approximation as in reality, the river will adjust morphodynamically to the reduction in sediments, causing the eroded bed sediments to compensate for this deficit (Kondolf et al., 2014). Therefore, the reduction in sediment yield due to the dams will only be noticeable at the river mouth after a few decades. In addition to this, the reduction of flood peaks caused by the dams will also result in a decrease of the carrying capacity of the rivers, during the flood season. This effect has not been accounted for in these calculations but it could lead to an even more critical situation than the one

Table 5
Estimated trapping efficiency for the different dams.

Dam	River	Sub-basin	Trap efficiency Brune (1953) (%)	Trap efficiency Brown (1944) (%)
Ayme II	Bia	Comoe	97	96
Buyo	Sassandra	Sassandra	95	98
Kossou	Bandama	Bandama	85	59
Taabo	Bandama	Bandama	62	16
Akosombo	Volta	Volta	96	87
Barekese	Ofin	Pra	22	24
Bui	Volta	Mouhoun	94	99
Kpong	Volta	Volta	24	10
Nangbeto	Mono	Mono	97	94
Ilauko	Ilauko	Oueme	18	11

estimated. In order to properly account for these effects, detailed morphodynamic models of each river would be required.

3. Results

3.1. Wave modelling

The computed mean significant wave height along the entire coast is shown in Fig. 5. The figure shows how the wave height in general decreases from West to East with a minimum near the Keta Lagoon due to wave sheltering effect from the delta of the Volta River. The wave roses, for one of the nested wave models near the Keta lagoon, are also shown in Fig. 6. The information derived from the nested models can also be freely downloaded at the following link: http://opendap.deltares.nl/thredds/catalog/opendap/deltares/publications/Giardino_2017/catalog.html.

3.2. Sediment transport and shoreline evolution

3.2.1. Model validation. Period: 1985–2015

The sediment transport and shoreline evolution model was calibrated and validated using, as hindcast period, the time-span 1985–2015. In particular, the calibration procedure included a sensitivity analysis of predicted transport rates as a function of changes in sediment size and sediment transport formula. The simulated potential longshore transport derived from the calibrated model is shown in Fig. 7. In the same figure, values used for model calibration and derived both from literature and the shoreline analysis based on satellite images, have also been included. A zero value in shoreline position (X-axis) in the figure is located at the border between Liberia and Côte d'Ivoire.
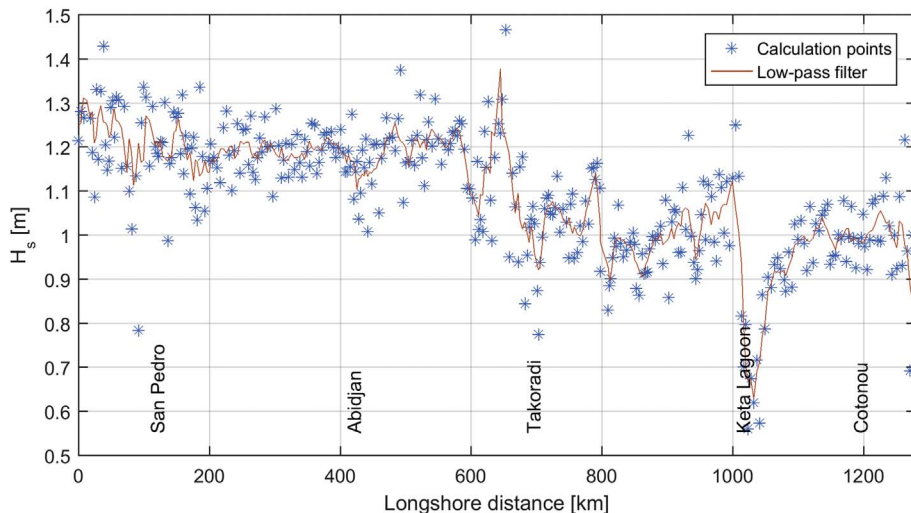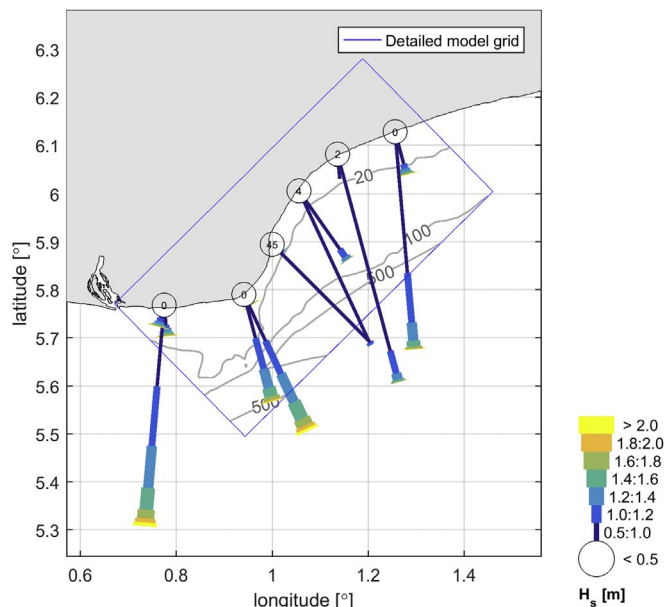

Fig. 6. Nearshore wave roses as computed by one of the nested SWAN models.

Model results indicated that the model is capable of capturing the large-scale potential transport rates and directions, which are in the same range compared to the data obtained from literature and the shoreline analysis. Most of the potential transport is eastward directed and ranges between 0 and 1.5 million m³/year. The transport direction reverses west of Cape Three Point due to the change in coastline orientation. When comparing with single validation points, we can see that the model represents accurately the transport rates west and east of Abidjan. Also the zero value in longshore transport in the eastern part of Côte d'Ivoire is well reproduced by the model. At the delta of the Volta river, the complete range of transport rates is covered by the model. Some differences can be observed at the port of Lomé and east of the Cotonou, with the model underestimating the longshore transport rates reported in literature and from the shoreline analysis. A possible reason for this discrepancy is that the values used for model validation actually estimate longshore transport rates as a result of shoreline changes induced by the presence of jetties, groynes, etc., however excluding the presence of other human activities (e.g. port dredging, leeside nourishments, sand mining from the beach, etc.). Other discrepancies may be due to the simplifications necessary in the development of the large-scale model schematization, meant to capture the
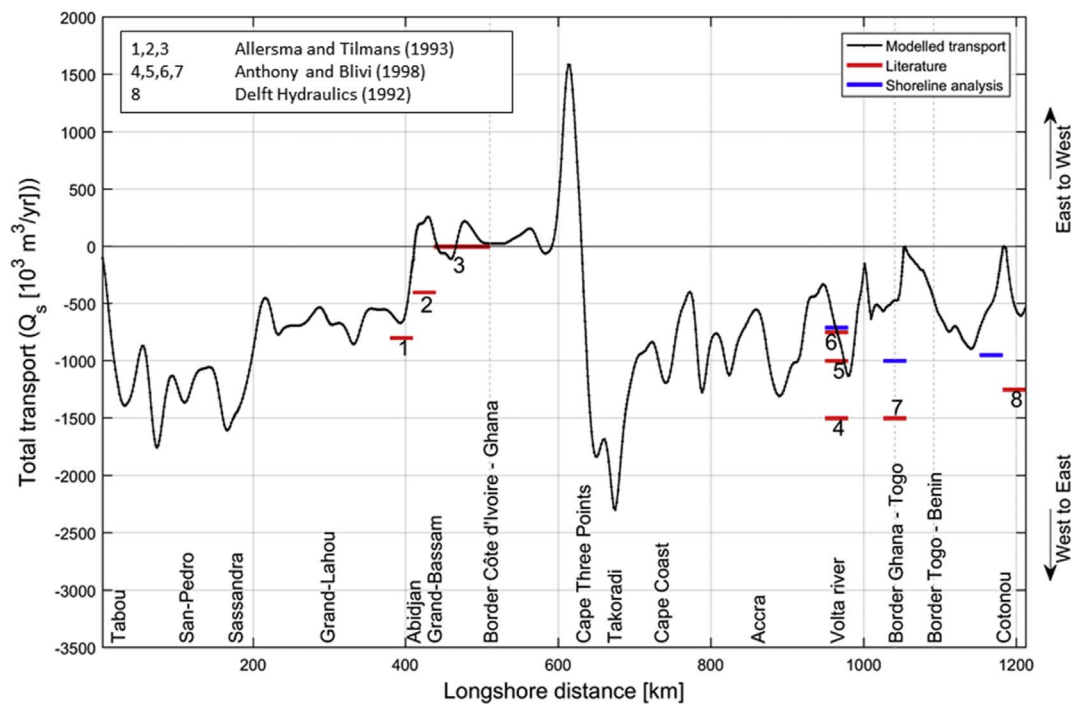

Fig. 5. Nearshore annual mean significant wave height as computed by all combined detailed models.

Fig. 7. Modelled longshore transport rates within the study area for the validation period. Horizontal lines represent the values derived from literature and the shoreline analysis and used for model calibration. The vertical dashed lines represent the boundaries between the countries.

large-scale sediment longshore transport along the West African coast. Among others, a uniformly applied sediment size and equilibrium profile, and a schematized coastline, from which small scale details have been removed.

At locations where pocket beaches are present, differences can be found between model results and actual transport rates. Small-scale pocket beaches are in fact not resolved by the model and are generally characterized by very small longshore transport rates. For example, the potential large computed transport rates at Cape Three Points, is related to the assumption of the fine grain size (D_{50} = 250 μm) and the unlimited supply of sand in the model. In reality, the coast here consists of rocky capes with alternating pocket beaches. The pocket beaches can be sheltered for wave impact due to the capes; moreover, the capes consist of rocky material. Therefore, the actual transport rates are expected to be smaller.

As an example, a comparison between measured shoreline changes based on analysis of satellite data and predicted changes based on numerical model results (in m/year), at the port of Lomé, are shown in Fig. 8.

The figure shows that the accretion up-drift, and the erosion down-drift of the jetty are both well reproduced by the model. The maximum simulated rate of accretion just up-drift of the jetty is 15 m/yr. According to Anthony and Blivi (1999), the maximum rate of accretion here was up to 1 km over a period of 30 years (i.e. 30 m/year). Therefore, at first sight, the modelled accretion rate appears to be underestimated. However, the modelled period here does not coincide with the time period considered in Anthony and Blivi (1999) (i.e. 1985–2015). In general, accretion tends to slow down when the shoreline reaches the top of the breakwater because of the increase in bypass around the port. Therefore, the maximum value of 15 m/yr seems appropriate. Just down-drift of the port, the coast is protected by a revetment at the location of the port, therefore any further potential erosion is now prevented and shifted downdrift. Further downdrift the rate of erosion is in the order of few meters per year, as also shown by the model.

Based on the presented validation results, it is concluded that the model has sufficient skill to investigate the scenarios outlined in Section 3.2.2.

3.2.2. Model prediction. Period: 2015–2045

3.2.2.1. Reference scenario. In this section, the calibrated model was used to assess the future shoreline evolution using, as a basis, the shoreline of 2015. The simulation was carried out for a period of 30 years (i.e. from 2015 until 2045) and assuming the presence of major structures along the coastline and on the main rivers, as in the current situation.

The results of this simulation are shown in Fig. 9. The Figure shows very similar patterns as already observed in Fig. 7 for the hindcast simulation. Potential transport rates are generally eastward directed and range approximately between 0 and 1.5 million m³/year. Near Cape Three Points, the longshore transport reverts direction (i.e. from East to West). The presence of the major ports (i.e. Abidjan, Lomé and Cotonou), with consequent coastline reorientation, results in a decrease of the transport rates which reduces to nearly zero in the vicinity of the ports. The effect of the major ports is assessed in the next section.

3.2.2.2. Effects of man-made interventions

3.2.2.2.1. Major ports. In order to assess the effect of the major ports on the shoreline evolution, a simulation was carried out in which all major ports were removed from the model, for the same simulated period (i.e. 2015–2045). The results of this simulation were compared to the reference scenario, in order to assess the relative impact that these ports have had on the shoreline evolution (Fig. 10). In particular, the panel above shows the longshore transport patterns both, for the reference situation and for the situation where ports have been removed. The panel below shows the relative difference between the two computed longshore transport rates. The simulation shows that the interruption of the longshore transport caused by the jetties of the ports in the reference situation is considerably reduced by removing those jetties. However, an interruption can still be noticed. This is due to the configuration of the coastline that has adjusted to the presence of the ports in the past decennia and which therefore will act as an obstruction to the longshore transport in the first decades after removing the ports. However, without the presence of these hard structures, the coastline will tend to smooth out in time and readapt to the pre-existing situation (i.e. before port construction).
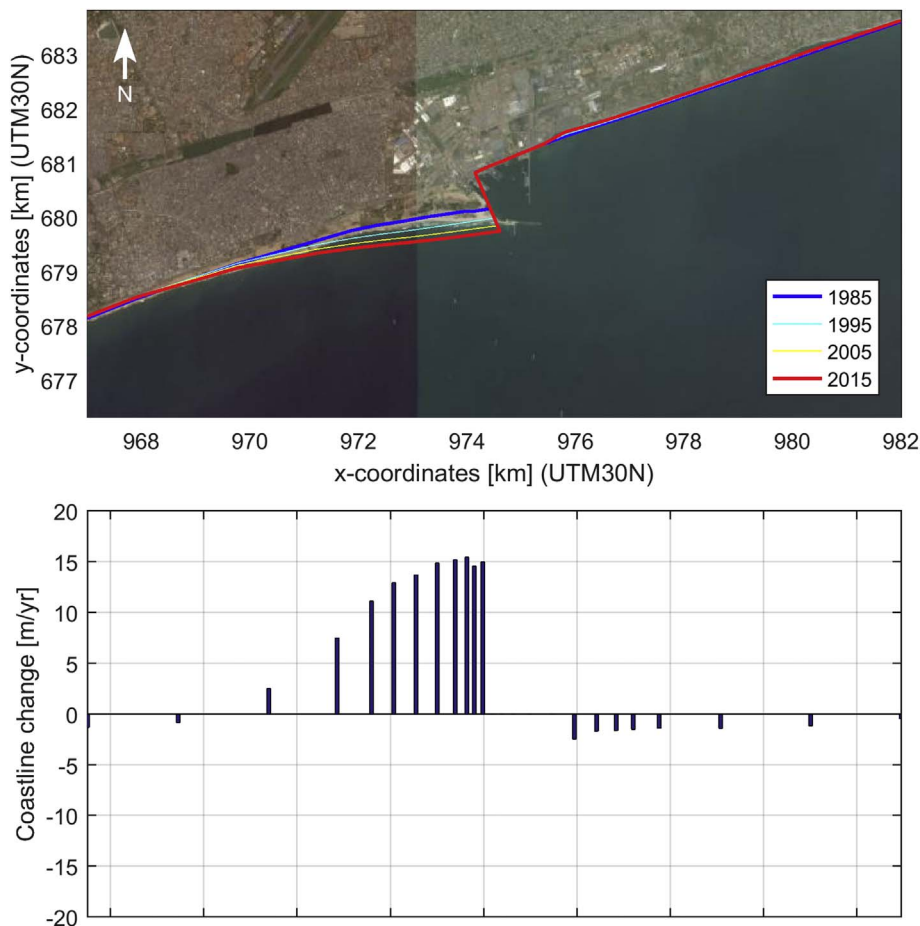
Fig. 8. Panel above: measured shoreline changes at the port of Lomé based on the analysis of satellite data. Panel below: computed shoreline changes (in m/year) based on numerical model results.

Although the port of Abidjan is quite large, the relative effect of the port on the longshore transport here is smaller. This is due to the relatively low estimated longshore transport rates at this location. On the contrary, the port of Lomé has a substantial effect on the transport rates. The transport rates are very large at this stretch of coast. Therefore the disturbance induced by the port leads to a large variation in the longshore transport patterns, both in magnitude and distance along the coast. The disturbance induced by the port to the longshore transport continues roughly for about 50 km (i.e. beyond the border between Togo and Benin). The port of Cotonou causes a substantial disturbance of the longshore transport pattern as well, however more limited in space, extending for about 30 km.

The model was also used to assess the expected shoreline changes resulting from the removal of the major ports (Fig. 11). This hypothetical calculation was carried out to describe implicitly, the present impacts of the ports on the shoreline. These results can also provide an indicative evaluation of the effects of the use of a sediment by-pass system that could bring the sediments from one side to the other one of each port.

Fig. 11 shows that by removing the ports, the coastline will start eroding updrift of the former ports and the increased sediment availability will cause accretion at the down-drift side. The coastline will continue to adjust to the new equilibrium situation until there are (hardly) any gradients in the transport pattern. This new situation will be close to the situation before port construction. The adjustment will occur at a quick rate of approximately 10–20 m/yr. The adjustment of the coast down-drift of the port of Lomé, for example, continues for nearly 50 km, in accordance to the changes in longshore transport as shown in Fig. 10.

3.2.2.2.2. Major river dams. In order to assess the effect of river damming on predicted shoreline changes, a scenario was simulated assuming the absence of dams on the rivers (i.e. no sediment trapping) and compared to the reference scenario.

The resulting longshore transport pattern is shown in Fig. 12 (top panel). The bottom panel shows the difference in transport between this scenario and the reference model. It can be seen that the increased sediment availability cause a decrease in the magnitude of transport updrift of the river outlets, and an increase downdrift, due to the tendency of delta formations at the mouths of the rivers. The difference between the two curves shows that changes are the largest at the Volta River. The sediment yield at the Volta catchment is in fact the largest. Moreover, the presence of several dams in the present situations blocks a large amount of the total sediment yield. Therefore, the relative effect of removing the dams will be bigger at this location.

The relative coastline changes, with respect to the reference scenario, induced by the removal of the dams will reflect on a coastline progradation near the river outlets (Fig. 13). The accretion rate varies between 1 m/yr (Sassandra and Mono river) up to 6 m/yr (Volta river). The build-up of small deltas explains the reorientation of the coast and consequently the decrease in transport updrift of the deltas (Fig. 12). However, in reality, the processes of delta formation will also be influenced by cross-shore transport processes, which are not included in the present coastal evolution model set-up.

3.2.2.3. Effects of climate change. Period 2070–2100. The effects of climate change on the coastal sediment budget are compared with the reference coastal evolution model. In particular, the following scenarios are simulated, as summarized in Table 3:

- Effects of sea level rise and changes in offshore wave climate on longshore transport patterns and resulting shoreline variations.
- Effects of changes in the hydrology at the river catchments (i.e. temperature and precipitation) and resulting shoreline variations.
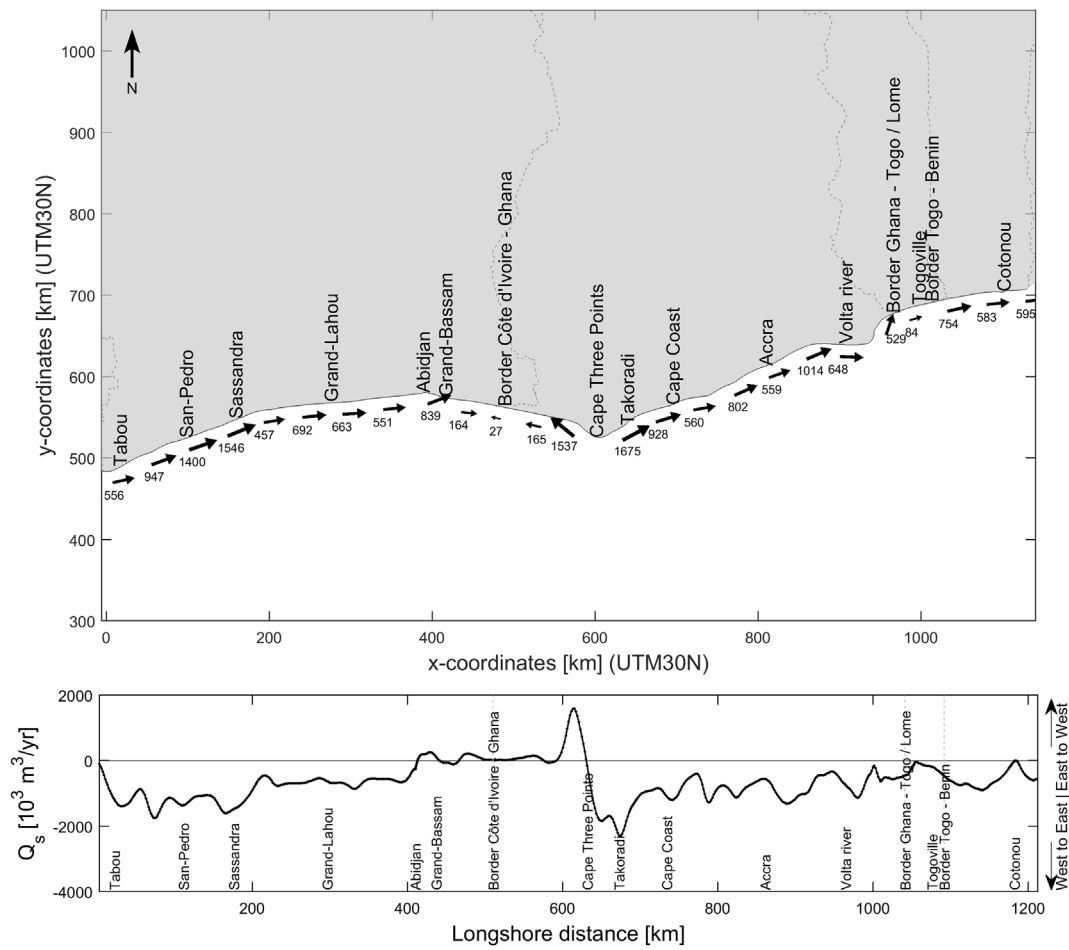- Effect of area loss due to sea level rise.

Fig. 9. Predicted longshore sediment transport and direction for the reference scenario. Values provided in thousands m³/year.
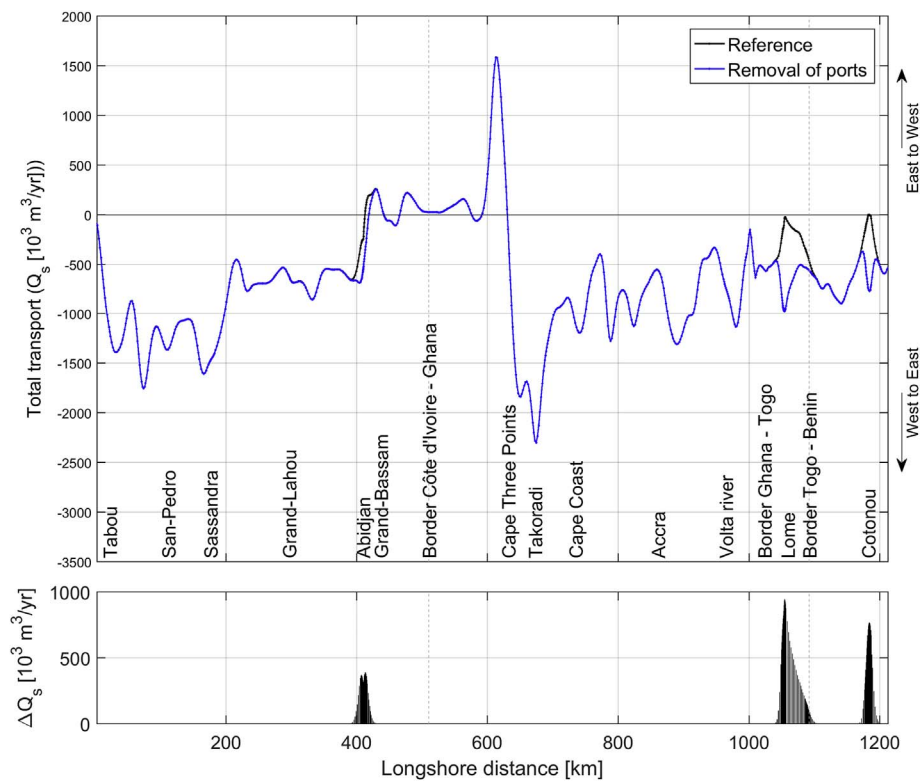

Fig. 10. Panel above: longshore transport patterns for the reference situation (in black) and after removal of the major ports (in blue). Panel below: relative absolute difference in modelled transport with respect to the reference situation. (For interpretation of the references to colour in this figure legend, the reader is referred to the Web version of this article.)
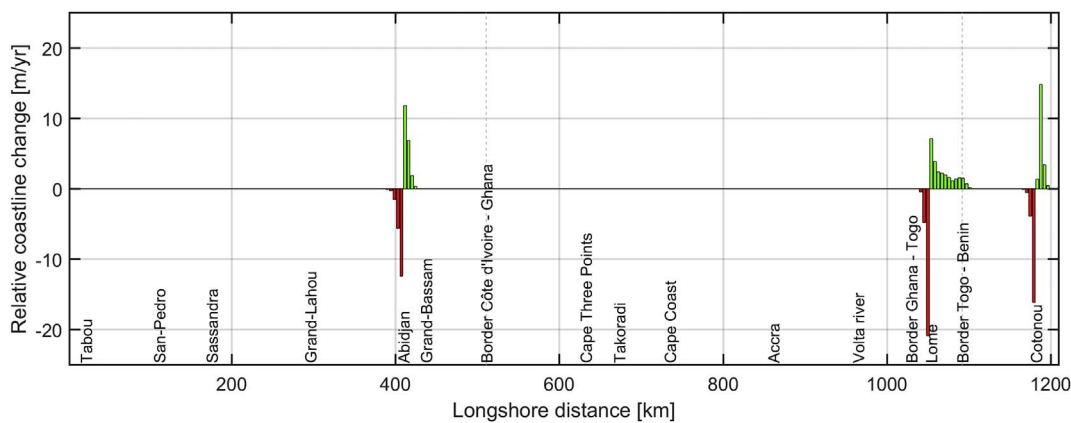
Fig. 11. Relative coastline changes for the hypothetical situation where the major ports are removed. Red indicates erosion, green indicates accretion. Relative changes are with respect to the reference situation. (For interpretation of the references to colour in this figure legend, the reader is referred to the Web version of this article.)

3.2.2.3.1. Changes in SLR and offshore wave climate. Climate change scenarios from the end of the century (2070–2100, Section 2.3.4 and 2.3.5) are used in this section to force shoreline model runs for thirty years, to be compared with the thirty years reference model simulations.

The schematization of the coastline and the forcing locations in the shoreline model are the same as for the 2015 reference model. However, new wave model runs were carried out to account for the simulated climate change conditions which therefore will result into new wave forcing conditions for the shoreline model.

The changes in longshore transport pattern resulting from the two SLR scenarios of +0.3 m and +1.0 m and including a change in the offshore wave condition (+3% in wave height; clockwise rotation of 2°) are shown in Fig. 14.

It can be clearly seen that the magnitude of the overall potential transport pattern becomes larger for both scenarios with respect to the reference case. This effect is mainly caused by the rotation of the wave climate and the increase in wave height of 3%. The relative effect of

SLR from 0.3 m to 1.0 m on longshore transport patterns is minor and not larger than 20–30 m³/yr.

The increase in transport rates varies at different locations along the entire West African coast (Fig. 14, panel below). As a consequence, gradients in longshore transport will also change, which in turns will cause an additional response (i.e. accretion or erosion) of the shoreline.

The predicted relative coastline changes, after a 30 year simulation period, are shown in Fig. 15. As expected, the rotation of the wave climate will induce an alternation of erosive and accretive trends, additionally to the reference situation, and with value up to about 2 m/yr, but generally lower than 1 m/yr. Maximum values can be seen near ports and at the Volta river delta. In fact, the wave sheltering effect induced by the presence of the ports and the river delta at these locations will be relatively larger due to the rotation of the wave climate, therefore inducing larger gradients.

It is important to stress that, changes in mean sea level, will also have a feedback on the local hydrodynamic conditions, in particular in shallow water, which in turn will result into additional changes on the
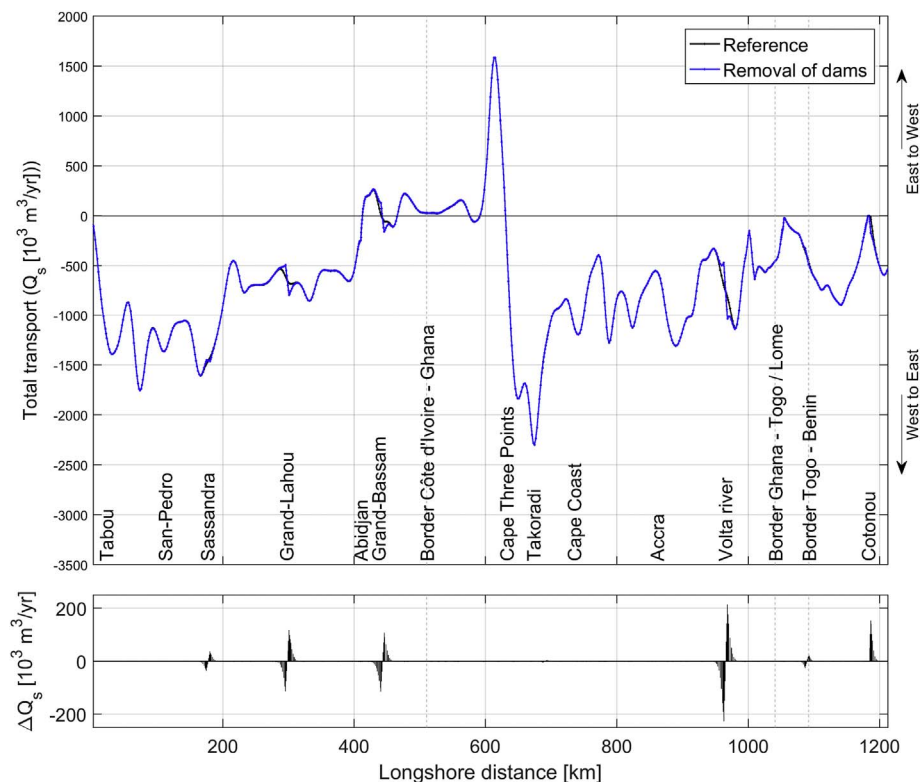

Fig. 12. Panel above: longshore transport for the reference situation (in black) and for the case after dam removal (in blue). Panel below: relative absolute difference in modelled transport after dam removal with respect to the reference situation. (For interpretation of the references to colour in this figure legend, the reader is referred to the Web version of this article.)
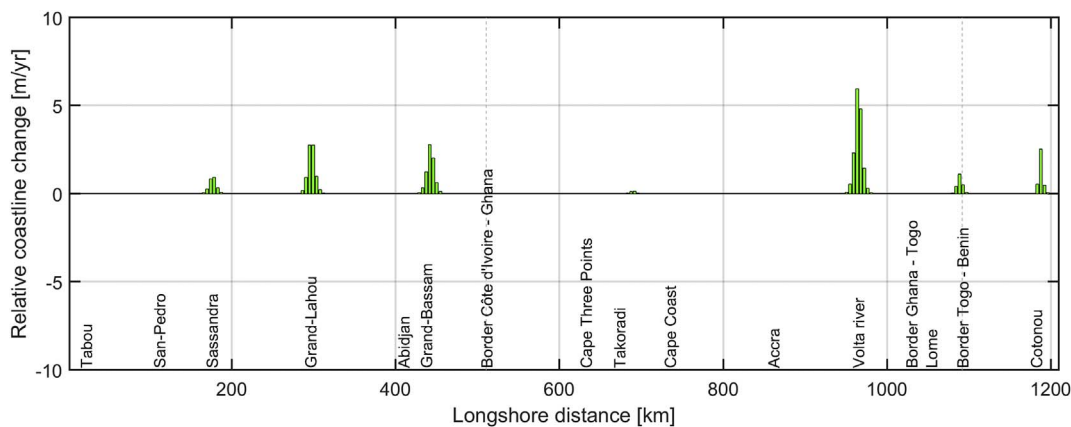
Fig. 13. Relative coastline changes for the hypothetical situation where the dams are removed from the rivers. Relative changes are with respect to the reference situation.

local morphodynamics. As the study focuses on a large-scale, long-term assessment, this effect is not taken into account in the analysis.

3.2.2.3.2. Changes in sediment yield from the rivers. In this section, the effect of climate change on the sediment yield at the river catchments and the relative effects on predicted shoreline changes is simulated. In particular, a relative 6 °C increase in temperature, and a +20% or −20% change in precipitation were taken into account. The climate change scenarios (i.e. temperature and precipitation) are described in Section 2.3.6.

The longshore transport patterns for the reference situation and the two climate change scenarios are shown in Fig. 16 (panel above). It can be seen from this figure that the changes in sediment yield on the large scale sediment pattern are very minor and not noticeable. The changes have a local effect by inducing a sudden jump in the transport patterns near the river mouth (panel below). This jump is caused by the increased/decreased availability of sediments which can be transported along the coast, respectively for a case with a −20% and +20% of precipitation. It is important to mention that these results are based on

a direct coupling between changes at the river catchments due to climate change and the relative effects at the river mouth. In reality, as already observed for the river dams, there is a time lag which can last several decades between possible observed changes at the river catchments induced by climate change, and the morphological changes observed at the river mouth.

The local effects of a change in sediment yield on relative coastline changes (i.e. with respect to the reference situation) can be seen in Fig. 17. An increase in precipitation will decrease the sediment yield towards the coast (due to more vegetation) and will cause a general local regression of the coastline of maximum 30 cm/yr. The mechanism is vice versa for the situation with a −20% decrease in precipitation (where sediment yield will increase due to a decrease in vegetation).

The effect of the change in sediment yield is a maximum increased or decreased coastline change of approximately 30 cm per year. In the 30 year simulated period, this will contribute up to a maximum of 9 m of coastline retreat or advance. The effect of a change in sediment yield is almost a factor 10 smaller than the coastline changes induced by a
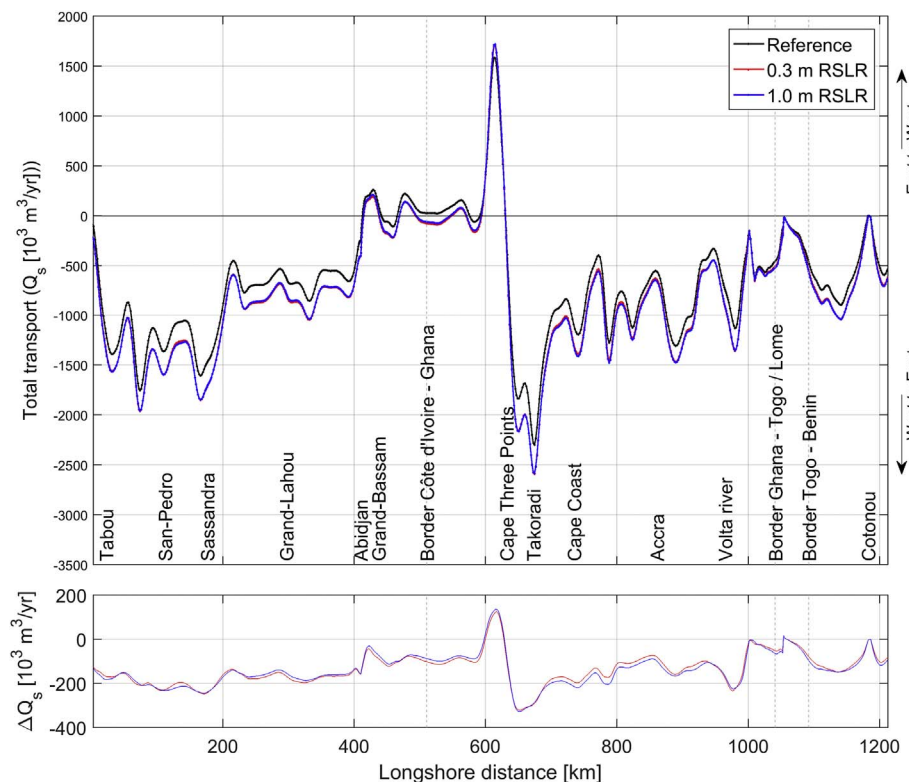

Fig. 14. Panel above: predicted longshore transport for the future scenarios, assuming an increase of 3% in significant wave height, a clockwise rotation of 2° in wave direction and an increase of +0.3 m (blue line) and +1.0 m (red line) in SLR. The black line indicates the longshore transport in the reference situation. Panel below: relative difference of the two scenarios with respect to the reference situation. (For interpretation of the references to colour in this figure legend, the reader is referred to the Web version of this article.)
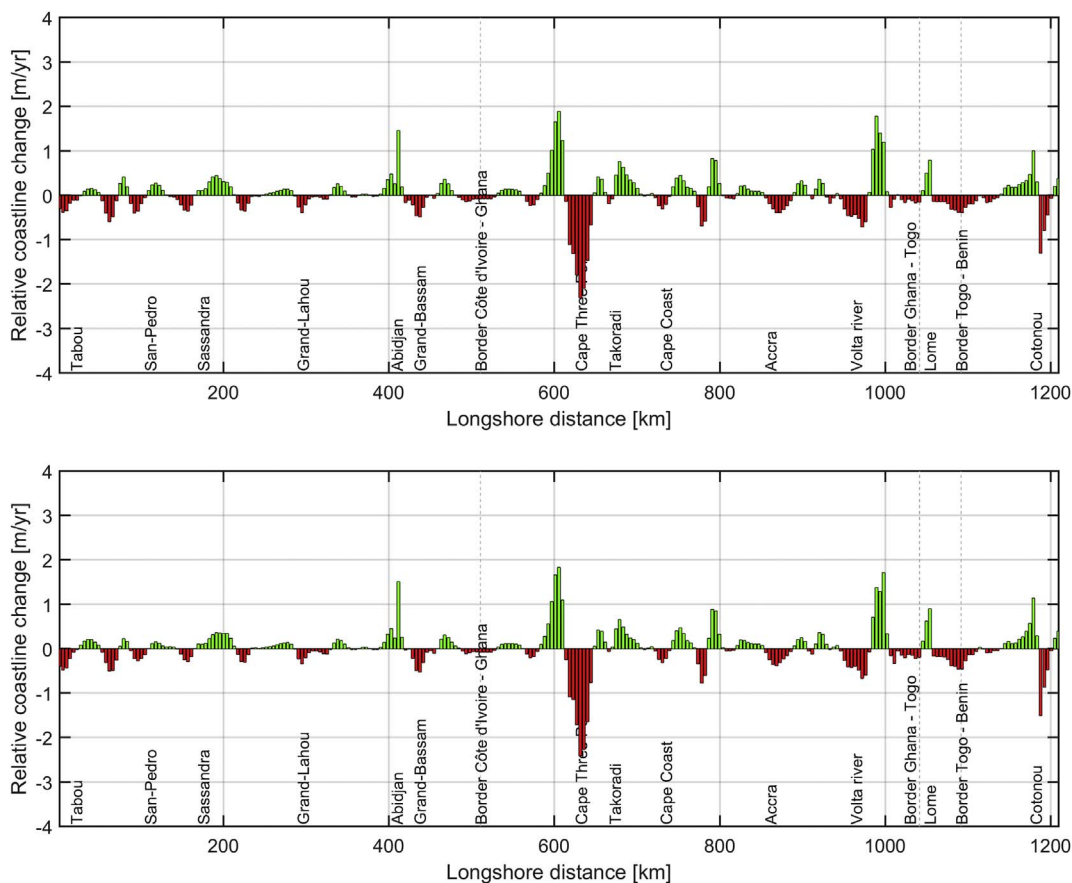
Fig. 15. Panel above: relative coastline changes for the future wave climate scenarios with an increase of 3% in significant wave height, a clockwise rotation of 2° in wave direction and a SLR of +0.3 m. Panel below: same figure as above but for a SLR of +1.0 m. Relative changes are with respect to the reference situation.
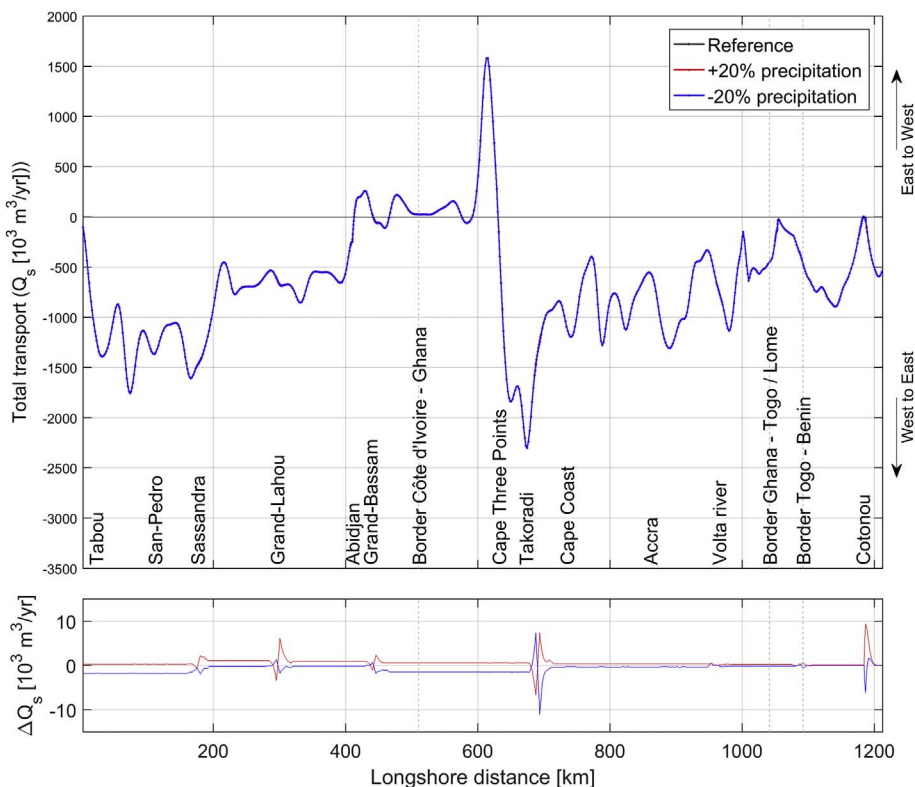

Fig. 16. Panel above: predicted longshore transport for the future scenarios, assuming a relative 6 °C increase in temperature, and a +20% (red line) or −20% (blue line) change in precipitation. Panel below: Relative difference of the two scenarios with respect to the reference situation. (For interpretation of the references to colour in this figure legend, the reader is referred to the Web version of this article.)
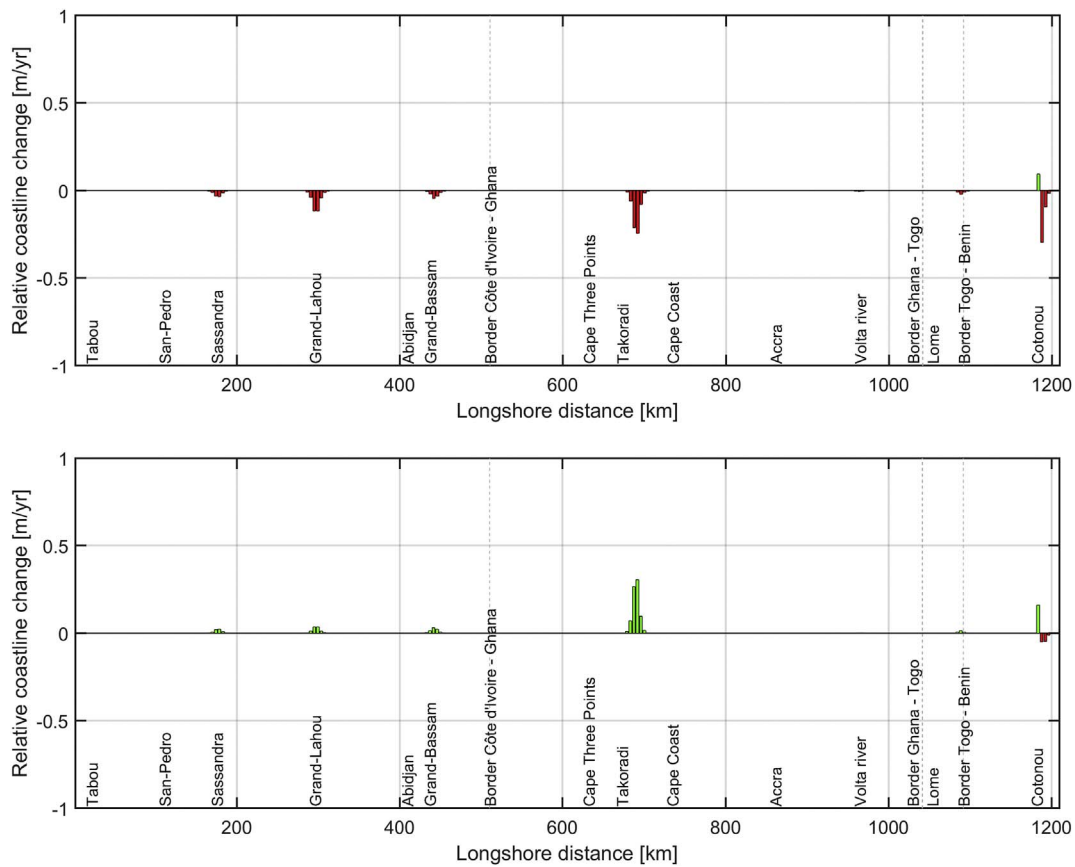
Fig. 17. Panel above: relative coastline changes for the future climate scenarios assuming an increase of 20% in precipitation. Panel below: same but assuming a decrease of 20% in precipitation. Relative changes are with respect to the reference situation.

change in sea level and wave direction. However, in reality both processes will affect the coastline at the same time and their effects will be combined.

3.2.2.3.3. Area loss due to SLR. In this section, the effect of coastal retreat and area loss induced by SLR is assessed by means of the very simplistic Bruun rule and applied on a theoretical Dean profile (Dean, 1977). Dean (1977) related the cross-shore water depth to the cross-shore distance, through a steepness factor depending on the sediment fall velocity. For the estimation of the cross-shore profile, a homogeneous sandy profile along the entire coast is used, with a mean grain size diameter of 250 μm and a depth of closure of 10 m. The predicted coastline retreat is then integrated along the length of the entire coastline. The increase in SLR is assumed to be linear over time until 2100. In reality, SLR rates are generally lower at present and they are assumed to increase at a faster rate towards the end of the century.

This may result in an overall area loss with a rate of about 0.25 m/year, assuming a relative SLR of 0.3 m by 2100, up to a rate of about 0.8 m/year assuming a relative SLR of 1.0 m by 2100. The area losses induced by the different contributions analyzed as part of this study are also summarized in Table 6.

4. Discussions

The results from the numerical modelling study presented in this paper have provided a quantification of the potential sediment transport and sediment budget along the West Africa coast in the current situation. Computed values are in line with values previously derived from literature for the different countries (e.g. Allersma and Tilmans (1993); Anthony (1995); Tilmans et al. (1995), Anthony and Blivi (1999); Almar et al. (2015). Moreover, the different scenarios have highlighted the inter-connection between the coastal systems and the

rivers. In addition, climate change effects, either at the river catchments or at sea, can have an effect on the overall sediment budget.

The different mechanisms have been assessed separately as part of different scenario runs. In reality, the different processes all contribute, at the same time, to the total longshore transport and shoreline changes. In Table 6, the net area loss and area gain per year over a 30 year period, over the entire region, resulting from the different contributions has been quantified. It is important to mention that, with the exception of the case of coastline retreat due to SLR, for all the other cases, coastline erosion at some locations is generally compensated by accretion at other locations. However, the focus of policy makers and local stakeholders is generally on the area loss, which may affect local population, infrastructures, and economic development at the areas affected by erosion. As an example, the effect of a major port is to cause erosion at the down-drift side of the port and accretion at the up-drift side.

The table shows that the effect of area loss due to the major ports is approximately in the same order of magnitude than the effect of coastal retreat due to SLR, when considering a SLR scenario of 0.3 m by 2100 (≈30 ha/year). However, if we consider a SLR of 1.0 m, the contribution of coastline retreat due to sea level rise, will be the largest of all the others (≈100 ha/year). The contributions due to changes in wave climate resulting from a lower wave dissipation (due to SLR), increase in offshore wave height and change in incoming wave direction will lead to an additional area loss of ≈15–20 ha/year. The removal of dams may lead to an increase in the amount of sediment towards the coast and therefore a gain in coastal area (≈20 ha/year). A decrease in precipitation will not result in any coastline losses (only accretion), while an increase in precipitation may result in an area loss of ≈1 ha/year as a result of more dense vegetation at the river catchments, which will retain more sediments.

Table 6
Areal land loss due to erosion and coastal retreat as a result of each different process with respect to the reference model.

	Simulation	Total area loss (ha/year)	Total area gain (ha/year)
Man-made intervention	Effects of major ports	33	33
	Removal of major river dams	0	18
Climate change	Change in wave condition due to: a) 0.3 m RSLR + b) change in offshore wave climate	18	19
	Change in wave condition due to: a) 1.0 m RSLR; b) change in offshore wave climate	18	18
	Change in hydrology due to: a) +20% precipitation; b) +6° temperature	1	0
	Change in hydrology due to: a) −20% precipitation; b) +6° temperature	0	1
	Coastline retreat due to 0.3 m SLR (Bruun rule)	30	0
	Coastline retreat due to 1.0 m SLR (Bruun rule)	100	0

However, it is important to emphasize that these values are only indicative and are meant to provide an order of magnitude of the contribution to coastal erosion/accretion induced by the existing anthropogenic interventions and climate change scenarios. Therefore, the values should not be interpreted as exact values rather they provide an indication of their relative contribution and trends. Moreover, the coastline erosion on smaller scales will be influenced by site specific processes which are not taken into account in those large-scale and long-term assessments (see e.g. Hinkel et al., 2012). Also, the climate change scenarios used in this paper, include a number of worst-case scenarios (e.g. sea level rise, precipitation, temperature).

Finally, it is important to mention that, as part of this study, only the effects of the major man-made interventions (i.e. ports and river dams) which are currently present in the region have been assessed. Nevertheless, other structures of smaller dimensions are present in the current situation. In addition, as a result of the economic growth in the region, new plans are being developed to construct or extend some of the structures already present in the region. Those new infrastructures may lead to additional erosion in the future, when no proper measures will be implemented to counteract any potential side-effect. Among possible measures which could be adopted to restore the natural sediment balance: the implementation of sediment by-passing systems around the major ports, the re-use of dredged sediments from the access channels towards the ports and a reduction in sedimentation in the upstream dams. The present study has shown implicitly the potential benefits that could arise from the implementation of such measures, such as accretion at the lee-side of the major ports, after implementation of sediment by-passing systems around ports, or sedimentation at the river deltas, after reduction of the trapping efficiency at the river dams.

An alternative to restore the natural sediment budget along the coast is the use of sediment resources from deeper water, which is currently barely used at the West African coast. Offshore sediment resources could be in fact used for the implementation of sand nourishments at locations affected by erosion.

Technical solutions to the coastal erosion problem will also require complementary actions at the governance level. A high priority action will be the involvements of the most relevant stakeholders, within the countries and from the different countries, working together towards the definition of an integrated regional sediment management plan for the region.

5. Conclusions: towards an integrated regional sediment management plan

In this study, a consistent large-scale sediment budget for the coastline of Côte d'Ivoire, Ghana, Togo and Benin has been derived. This has been used to quantify the effects of different human interventions (i.e. major ports and river dams) on the coastal system and possible trans-boundary implications. The effect of climate change (i.e. increase in wave conditions, change in wave direction, SLR, and variations in temperature and precipitation at the river catchments) on the large scale sediment transport and consequent shoreline changes has also been analyzed.

The study has shown how some of the man-made interventions have had major effects on the large-scale sediment budget and consequent shoreline changes. As an example, the effect of the port of Lomé in Togo may extend up over 50 km, therefore beyond the border between Togo and Benin. Large amount of sediments are also retained behind river dams. The modelling system has shown that, if this sediment yield would be released from the dams, this could promote sediment accretion at the coast up to several meters per year. This is especially evident at the Volta river, which used to carry the highest sediment discharge at the coast, and where major river dams (e.g. the Akosombo dam) have now been built.

The effects of the current major ports on coastal erosion will be of the same order of magnitude as the effect of SLR, when considering lower SLR scenarios (RCP 4.5). However, SLR may overrule the effect of the other man-made interventions by the end of the century if considering the largest predicted sea level rise scenarios (RCP 8.5). This of course will depend on the actual SLR, as well as the possible developments of new structures along the coast and at the river basins, which may lead to additional erosion.

Possible changes in offshore wave conditions induced by climate change (i.e. wave height and incoming wave direction) may lead to changes in gradients of longshore transport, which in turns will cause a response (i.e. local accretion or erosion) of the shoreline up to 1–2 m/y. Finally, possible changes at the river catchments related to climate change (e.g. changes in precipitation or temperature) will only result into localized changes at the coastline.

The study clearly pointed out the interdependency between different interventions, either along the rivers or at the coast on the overall sediment budget. As these effects do not pay heed to geographical boundaries and considering the severity of the current coastal erosion problems in the region, it is highly advisable that a large-scale integrated sediment management plan is set-up. Such a plan should, on the one hand, aim at creating awareness between policy makers in the different countries about current and future challenges in relation to sediment management and the need of a common strategy to tackle those problems. On the other hand, the plan should provide the basis for the development of a common policy in relation to sediment management, with identification of common objectives, priorities, strategies and timeframes to achieve those. The fragmentation of actors and responsibilities between West African countries, and even within the same country, has hampered the planning of effective and sustainable solutions for decades. Although the compliance with legal and regulatory frameworks is obviously a challenge that pertains to state sovereignty, the building of consensus and of a common strategy to deal with coastal erosion are necessary mechanisms to support the implementation of this plan. This sediment management plan could be supported by the use of a common, and cross-boundary, numerical modelling study as described in the paper, and implemented following a

collaborative modelling approach (Basco-Carrera et al., 2017).

Complementary to actions at the governance level, the plan should define how those strategies could be implemented in practice (e.g. how much sediment is required to tackle coastal erosion, where and how much sediment resources are available etc.). Finally, the plan should promote the development of a regional monitoring system to evaluate the efficiency of the coastal erosion policy and of the planned interventions, building upon already existing studies and initiatives (e.g. UEMOA, 2011; 2015). The setting up of such a sediment management plan is especially important, in view of the new expected infrastructural developments in the region, which may worsen the already critical current situation.

Acknowledgements

References

Abe, J., 2005. Contribution a la Connaissance de la Morphologie et de la Dynamique Sedimentaire du Littoral Ivoirien (Cas du Littoral d'Abidjan). Essais de modelisation en vue d'une gestion rationnelle. These de Doctorat d'Etat ès Sciences Naturelles. Thesis. Université de Cocody, Abidjan.

Allersma, E., Tilmans, W.M.K., 1993. Coastal conditions in West Africa – a review. J. Ocean Coast. Manag. 19, 199–240.

Almar, R., Kestenare, E., Reyns, J., Jouanno, J., Anthony, E.J., Laibi, R., Hemer, M., Du Penhoat, Y., Ranasinghe, R., 2015. Response of the Bight of Benin (Gulf of Guinea, West Africa) coastline to anthropogenic and natural forcing. Part 1: wave Climate variability and impacts on the longshore sediment transport. J. Cont. Shelf Res. 110, 48–59.

Anthony, E.J., 1995. Beach-ridge progradation in response to sediment supply: examples from West Africa. J. Mar. Geol. 129, 175–186.

Anthony, E.J., Blivi, A.B., 1999. Morphosedimentary evolution of a delta-sourced, drift-aligned sand barrier-lagoon complex, western Bight of Benin. Mar. Geol. 158, 161–176.

Anthony, E.J., Almar, R., Aagaard, T., 2016. Recent shoreline changes in the Volta River delta, West Africa: the roles of natural processess and human impacts. Afr. J. Aquat. Sci. 41 (1), 81–87.

Basco-Carrera, L., Warren, A., van Beek, E., Jonoski, A., Giardino, A., 2017. Collaborative modelling or participatory modelling? A framework for water resources management. J. Environ. Model. Softw. 91, 95–110.

Boateng, I., 2012. An application of GIS and coastal geomorphology for large scale assessment of coastal erosion and management: a case study of Ghana. J. Coast. Conserv. 16, 383–397.

Booij, N., Ris, R.C., Holthuijsen, L.H., 1999. A third-generation wave model for coastal regions: 1. Model description and validation. J. Geophys. Res. 104, 7649–7666.

Brown, C.B., 1944. Discussion of sedimentation in reservoirs. In: In: Witzig, J. (Ed.), Proc. of the American Society of Civil Engineers, vol. 69. pp. 1493–1500.

Brune, G.M., 1953. Trap efficiency of reservoirs. Trans. Am. Geophys. Union 34 (3), 407–418.

Bruun, P., 1962. Sea level rise as a cause of shore erosion. J. Waterw. Harb. Div. ASCE 88, 117–130.

Christensen, J.H., Christensen, O.B., 2007. A summary of the PRUDENCE model projections of changes in European climate by the end of this century. Clim. Change 81 (1), 7–30.

Cooper, J.A.G., Pilkey, O.H., 2004. Sea-level rise and shoreline retreat: time to abandon the Bruun Rule. Global Planet. Change 43, 157–171. http://dx.doi.org/10.1016/j.gloplacha.2004.07.001.

Dean, R.G., 1977. Equilibrium Beach Profiles: U.S. Atlantic and Gulf Coasts. Department of Civil Engineering, Ocean Engineering Report N° 12, University of Delaware, Newark, Delaware.

Dee, D.P., Uppala, S.M., Simmons, A.J., Berrisford, P., Poli, P., Kobayashi, S., Andrae, U., Balmaseda, M.A., Balsamo, G., Bauer, P., Bechtold, P., Beljaars, A.C.M., van de Berg, L., Bidlot, J., Bormann, N., Delsol, C., Dragani, R., Fuentes, M., Geer, A.J.,

Haimberger, L., Healy, S.B., Hersbach, H., Hólm, E.V., Isaksen, L., Kållberg, P., Köhler, M., Matricardi, M., McNally, A.P., Monge-Sanz, B.M., Morcrette, J.-J., Park, B.-K., Peubey, C., de Rosnay, P., Tavolato, C., Thépaut, J.-N., Vitart, F., 2011. The ERA-Interim reanalysis: configuration and performance of the data assimilation system. Q.J.R. Meteorol. Soc. 137, 553–597. http://dx.doi.org/10.1002/qj.828.

Degbe, C.G.E., 2009. Géomorphologie et érosion côtière dans le Golfe de Guinée. Mémoire de Master 2. CIPMA, Université d'Abomey-Calavi (UAC), Cotonou, pp. 100.

Deltares, 2011. UNIBEST-CL+ Manual. Manual for Version 7.1 of the Shoreline Model UNIBEST-CL+. Delft, The Netherlands.

Dendy, F.E., Bolton, G.C., 1976. Sediment yield-runoff-drainage area relationships in the United States. J. Soil Water Conserv. 31 (6), 264–266.

Donchyts, G., Baart, F., Winsemius, H., Gorelick, N., Kwadijk, J., Van De Giesen, N., 2016. Earth's surface water change over the past 30 years. Nat. Clim. Change 6, 810–813. http://aqua-monitor.deltares.nl.

Giardino, A., di Leo, M., Bragantini, G., de Vroeg, H., Tonnon, P.K., Huisman, B., de Bel, M., 2015. An integrated sediment management scheme for the coastal area of Batumi (Georgia). In: Proceedings of the Medcoast Conference, Varna, Bulgaria.

Giardino, A., Schrijvershof, R., Brière, C., Nederhoff, C.M., Tonnon, P.-K., Caires, S., 2017. Human Interventions and Climate Change Impacts on the West African Coastal Sand River. World Bank report, Washington, DC.

Hemer, M.A., Fan, Y., Mori, N., Semedo, A., Wang, X.L., 2013. Projected changes in wave climate from a multi-model ensemble. J. Nat. Clim. Change 3, 471–476 DOI:10.1038.

Hinkel, J., Brown, S., Exner, L., Nicholls, R.J., Vafeidis, A.T., Kebede, A.S., 2012. Sea-level rise impacts on Africa and the effects of mitigation and adaptation: an application of DIVA. J. Reg. Environ. Change 12 (1), 207–224.

Holthuijsen, L.H., Booij, N., Ris, R.C., 1993. A spectral wave model for the coastal zone. In: Proceedings 2nd International Symposium on Ocean Wave Measurement and Analysis, New Orleans, Louisiana, July 25–28, 1993, pp. 630–641 New York.

IPCC AR5 WG1, 2013. In: Stocker, T.F. (Ed.), Climate Change 2013: the Physical Science Basis. Working Group 1 (WG1) Contribution to the Intergovernmental Panel on Climate Change (IPCC) 5th Assessment Report (AR5). Cambridge University Press.

Jeuken, A., Bouaziz, L., Corzo, G., Alfonso, L., 2016. Analyzing needs for climate change adaptation in the magdalena river basin in Colombia. In: Filho, W.L., Musa, H., Cavan, G., O'Hare, P., Seixas, J. (Eds.), Climate Change Adaptation, Resilience and Hazards. Climate Change Management, Springer International Publishing, pp. 329–344. http://link.springer.com/chapter/10.1007/978-3-319-39880-8_20, Accessed date: 26 September 2016.

Jonah, F.E.J., Adjei-Boateng, D., Agbo, N.W., Mensah, E.A., Edziyie, R.E., 2015. Assessment of sand and stone mining along the coastline of Cape Coast, Ghana. J. Ann. GIS 21 (3), 223–231.

Kaki, C., Laïbi, R.A., Oyédé, L.M., 2011. Evolution of Beninese coastline from 1963 to 2005: causes and consequences. Br. J. Environ. Clim. Change 1 (4), 216–231.

Kondolf, G.M., Gao, Y., Annandale, G.W., Morris, G.L., Jiang, E., Zhang, J., Cao, Y., Carling, P., Fu, K., Guo, Q., Hotchkiss, R., Peteuil, C., Sumi, T., Wang, H.-W., Wang, Z., Wei, Z., Wu, B., Wu, C., Yang, C.T., 2014. Sustainable sediment management in reservoirs and regulated rivers: experiences from five continents. Earth's Future 2, 256–280. http://dx.doi.org/10.1002/2013EF000184.

Laïbi, R.A., Anthony, E.J., Almar, R., Castelle, B., Senechal, N., Kestenare, E., 2014. Longshore drift cell development on the human-impacted Bight of Benin sand barrier coast, West Africa. J. Coast. Res. 78–83 Special Issue, No. 70.

Lopez Lopez, P., Wanders, N., Schellekens, J., Renzullo, L.J., Sutanudjaja, E.H., Bierkens, M.F.P., 2015. Improved large-scale hydrological modelling through the assimilation of streamflow and downscaled satellite soil moisture observations. Hydrol. Earth Syst. Sci. Discuss. 12, 10559–10601. http://dx.doi.org/10.5194/hessd-12-10559-2015.

Lu, J., Sun, G., McNulty, S.G., Amatya, D.M., 2005. A comparison of six potential evapotranspiration methods for regional use in the southern United States. JAWRA J. Am. Water Resour. Assoc. 41, 621–633. http://dx.doi.org/10.1111/j.1752-1688.2005.tb03759.x.

Ly, C.K., 1980. The role of the Akosombo Dam on the Volta river in causing erosion in central and eastern Ghana (West Africa). J. Mar. Geol. 35, 323–332.

Ranasinghe, R., Callaghan, D., Stive, M.J.F., 2012. Estimating coastal recession due to sea level rise: beyond the Bruun rule. Clim. Change 561–574. http://dx.doi.org/10.1007/s10584-011-0107-8.

Schellekens, J., 2013. Open Streams: Wflow Documentation (Release 0.91).

Sultan, B., Roudier, P., Quirion, P., Alhassane, A., Muller, B., Dingkuhn, M., Ciais, P., Guimberteau, M., Traore, S.B., Baron, C., 2013. Assessing climate change impacts on sorghum and millet yields in the Sudanian and Sahelian savannas of West Africa. Environ. Res. Lett. 8 (1), 014040.

Syvitski, J.P.M., Kettner, A.J., Overeem, I., Hutton, E.W.H., Hannon, M.T., Brakenridge, G.R., Day, J., Vörösmarty, C., Saito, Y., Giosan, L., Nicholls, R.J., 2009. Sinking deltas due to human activities. J. Nat. Geosci. http://dx.doi.org/10.1038/NGEO629.

Tilmans, W.M.K., Jakobsen, P.R., LeClerc, J.P., 1991. Coastal erosion in the Bight of Benin. In: Tilmans, W.M.K., Jakobsen, P.R., LeClere, J.P. (Eds.), A Critical Review, Technical report. Delft, The Netherlands.

Tilmans, W.M.K., de Vroeg, H.H., Leclerc, J.-P., 1995. Coastal protection at Cotonou, Benin. In: International Conference on Coastal and Port Engineering in Developing Countries, vol. 1. pp. 171–184 Brazil.

UEMOA, 2011. Regional Study for Shoreline Monitoring and Drawing up a Management Scheme for the West African Coastal Area.

UEMOA, 2015. Update of the Regional Study for Shoreline Monitoring and Drawing up a Management Scheme for the West African Coastal Area.

UNEP, 1985. Coastal Erosion in West and Central Africa. UNEP Reg. Seas Report Study.

No. 67. UNEP, Geneva, pp. 237.

Van Rijn, 1984a. Sediment transport, Part I: bed load transport. J. Hydraul. Eng. ASCE 110 (10).

Van Rijn, 1984b. Sediment tranport, Part II: suspended load tranport. J. Hydraul. Eng. ASCE 110 (11).

Van Rijn, L.C., 2005. Principles of Sedimentation and Erosion Engineering in Rivers, Estuaries and Coastal Seas. Aqua Publications, The Netherlands.

Weedon, G.P., Balsamo, G., Bellouin, N., Gomes, S., Best, M.J., Viterbo, P., 2014. The WFDEI meteorological forcing data set: WATCH Forcing Data methodology applied to ERA-Interim reanalysis data. Water Resour. Res. 50, 7505–7514. http://dx.doi.org/10.1002/2014WR015638.

Wiafe, G., 2011. Coastal and Continental Shelf Processes in Ghana. Report. Department of Oceanography and Fisheries, University of Ghana.

Wognin, V., 2004. Caractérisation sédimentologique et hydrologique à l'embouchure du fleuve Bandama. Thèse doc. Unique Univ. Cocody, pp. 195.

Wognin, A.I.V., Coulibaly, A.S., Akobe, A.C., Monde, S., Aka, K., 2013. Morphologie du littoral et cinématique du trait de côte de Vridi à Grand Bassam (Cote d'Ivoire). J. Environ. Hydrol. 21 Paper 1.

World Bank, 2016. West Africa Coastal Areas Management Program. A Partnership for Saving West Africa's Coastal Assets. http://www.worldbank.org/en/topic/environment/brief/west-africa-coastal-areas.